Journal of Modern Computing and Engineering Research
JMCER
Volume 2025, p. 10-18
https://jmcer.org

Analysis of Photoplethysmogram (PPG) Signal Processing Results Compared to the Graph of Electrocardiogram (ECG)

Hilman Asyrafi[1], Sunarno[2], Memory Motivanisman Waruwu[3] and Rony Wijaya[4]
[1] *Department of Graphic Engineering, State Polytechnic of Creative Media, Makassar, Indonesia*
[2,3,4] *Department of Nuclear Engineering and Engineering Physics, Gadjah Mada University, Yogyakarta, Indonesia*

[1]hilman.asyrafi@polimedia.ac.id, [2] sunarno@ugm.ac.id,, [3] morymw@gmail.com,, [4] rwijaya80@gmail.com

Received: December 20, 2024 *Revised: March 29, 2025* *Accepted: April 8, 2025*

Abstract:
Electrocardiogram (ECG) and Photoplethysmogram (PPG) are tools that provide information about the cardiovascular system. The purpose of this study is to determine whether the ECG graph can be generated through the PPG data processing method. For this reason, a comparison is made between the feature value of normal ECG and the results of PPG signal processing. In this study, PPG signal processed is raw data measured with an easy pulse sensor on 25 normal subjects with the main method used is the second derivative of the PPG signal (SDPPG). There are 8 features used in this study (PR interval, P wave interval, QRS complex, RR interval, R wave amplitude, QT interval, T wave amplitude, and P wave amplitude) with comparison results between valid and invalid respectively is (15:10), (21:4), (0:25), (25:0), (25:0), (0:25), (25:0) and (25:0).These results indicate that the ECG graph can be generated through PPG signal processing provided that the features used are: P-wave interval, RR Interval, R-wave amplitude, T-wave amplitude, and P-wave amplitude.

Keywords: *ECG, PPG, Signal Processing, SDPPG, ECG Feature*

1 Introduction

Physiological rhythms or oscillations are the manifestation of a complex physiological system. The clinical community has long recognized that alterations in physiological rhythms are associated with disease and therefore have clinical value. Oscillations in cardiovascular systems are reflected in electrocardiogram (ECG) time series variability (Jelinek, Cornforth, and Khandoker 2017). An ECG is a graph of voltage with respect to time that reflects the electrical activities of cardiac muscle depolarization followed by repolarization during each heartbeat (Zheng et al. 2020). As a basic medical test in clinical settings, ECG plays a significant role in the diagnosis of cardiovascular diseases and is being used more frequently than before, since the incidence of cardiovascular diseases has been noticeably increased (Zeng 2015).

A standard ECG has 12 leads including 6 limb leads (I, II, III, aVR, aVL, aVF) and 6 chest leads (V1, V2, V3, V4, V5, V6) recorded from electrodes on the body surface (Zhang et al. 2021). Each lead looks at the electrical activities from a different angle. 12 leads are required for accurate diagnosis purpose; however, one lead can offer important information for quick and initial assessment of the patient (Hammad et al. 2018). In this study, lead II is used as a reference, this is because lead II can provide a good visualization of the most important waves in the ECG chart graph.

Despite the diagnostic value of ECG, its implementation faces several challenges in modern healthcare settings. Traditional ECG monitoring requires specialized equipment, trained personnel, and multiple electrode attachments, making it resource-intensive (Sattar and Chhabra 2025) and less suitable for continuous monitoring in non-clinical environments. These limitations have driven research toward alternative cardiovascular monitoring methods that are more accessible, cost-effective, and user-friendly for both clinical and home-based applications.

By convention, the main waves on the ECG are given the names P, Q, R, S, T and U (Figure 1). Each wave represents depolarization (‘electrical discharging’) or repolarization (‘electrical

Corresponding author: Hilman Asyrafi, hilman.asyrafi@polimedia.ac.id

recharging') of a certain region of the heart. The voltage changes detected by ECG machines are very small, being of the order of millivolts (Houghton 2019). Information related to the cardiovascular system can be obtained from the ECG graph in the form of wave duration and amplitude.

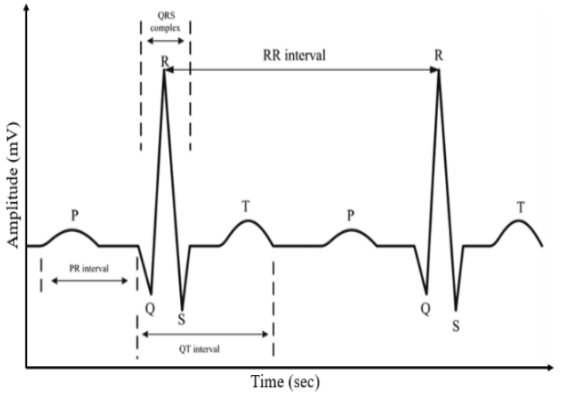

Figure 1: ECG Wave (Khincha et al. 2020)

One of the methods that provide valuable information related to the cardiovascular system is photoplethysmography (W.-F. Wang, Yang, and Wu 2018). PPG is a non-invasive and lowcost technique to measure blood volume change using an optical sensor (Hartmann et al. 2019). Compared to ECG, PPG offers several advantages: it requires only a single point of contact, uses inexpensive optical components, and can be easily integrated into wearable devices such as smartwatches (Scardulla et al. 2023). These characteristics position PPG as an attractive alternative for continuous cardiovascular monitoring, particularly in remote healthcare settings and for long-term patient management.

PPG measurements are carried out on body parts such as fingers, earlobe, and forehead (Castaneda et al. 2018). The main components of PPG are light sources and photodetectors. The light source emits light into the tissue and the photodetector measures changes in the light intensity of the body's tissues. The intensity of light captured by the PPG sensor will change along with changes in the volume of blood in the heart. The intensity of light captured by the PPG sensor will change along with changes in the volume of blood in the heart.

The PPG signal itself is quite simple (consists of four waveforms: onset, systolic, notch, dan diastolic) as shown in Figure 2 and not always informative, therefore most clinicians check the derivatives of PPG waveforms to better evaluate the changes in the waveforms (Elgendi, Liang, and Ward 2018). Previous research has explored relationships between PPG and ECG signals, including Heart-Rate Variability (HRV) and Pulse-Rate Variability (PRV) (Chen et al. 2021; Iozzia, Cerina, and Mainardi 2016), arrhythmia detection (Neha et al. 2021), hypertension assessment (Liang et al. 2018), and blood pressure estimation (Podaru and David 2020). However, these studies have typically focused on specific parameters rather than comprehensive ECG feature extraction.

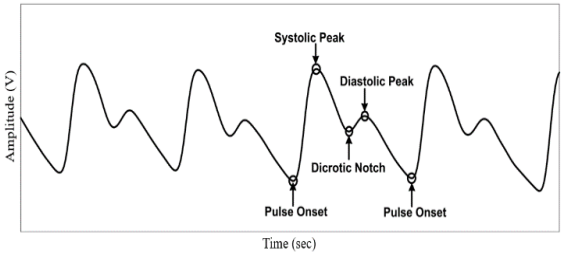

Figure 2: PPG Signal Waveform (Chakraborty et al. 2020)

Current approaches for deriving ECG features from PPG signals face several limitations. Time-domain methods often struggle with noise sensitivity and baseline wander (Mishra and Nirala 2020), frequency-domain approaches may lose temporal information critical for identifying specific waveform features and also preferred for short-term measurements (Ahmed, Bhuiyan, and Nii 2022), machine learning/deep learning while promising, frequently require large datasets (Benfenati et al. 2024; Wong et al. 2023) and reliability of the models can be affected by the quantity and diversity of the data (Zeynali et al. 2025). Additionally, most existing methods extract only rudimentary cardiovascular parameters from PPG (such as heart rate and pulse transit time) without capturing the detailed morphological information present in a full ECG waveform.

The main objective of this study is to determine whether the ECG graph can be generated through the PPG data processing method. Specifically, we investigate the second derivative of the PPG signal (SDPPG) as a means to reconstruct ECG-like waveforms and validate these against standard ECG features. By successfully deriving ECG parameters from PPG signals, this research could significantly reduce healthcare costs, enable more widespread cardiovascular monitoring through consumer wearables, and improve patient outcomes through earlier detection of cardiac abnormalities in non-clinical settings.

JMCER

2 Methodology

PPG signal processed is raw data measured with an easy pulse sensor on 25 normal subjects with a measurement duration of 10 seconds and sampling frequency of 100 Hz. Data processing is done using the python programming language. The stages of this research are shown in Figure 3.

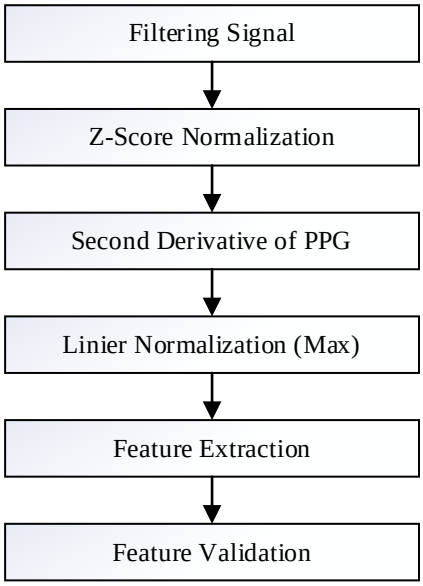

Figure 3: Stages of Research

2.1 Filtering Signal

Perform signal filter (Low-Pass Filter) to remove the noise of the PPG Signal [14]. The PPG signal is filtered in the range 0-10 Hz by applying the Infinite Impulse Response (IIR) filter which is expressed in the following equation (Krishnan 2021).

$$y(n) = \sum_{k=1}^{N} a_k x(n-k) - \sum_{l=0}^{M} b_l y(n-l) \qquad (1)$$

where $y(n)$ and $x(n)$ are output and input signals, respectively. The input filter coefficient a_k and the output filter coefficien b_l are obtained using the Chebyshev Type II method of order 4. This filter was specifically chosen for its steep roll-off characteristics and minimal phase distortion, which helps preserve the temporal relationships between waveform features - a critical factor when attempting to derive ECG-like features from PPG signals.

2.2 Z-Score Normalization

Z-score normalization aims to convert the data values into a common scale without distorting the difference in the range of values (Mukhyber, Abdulah, and Majeed 2021). The application of z-score normalization utilizes to adjust the ECG amplitude in the order of millivolts. The normalization of the z-score can be expressed in the following equation (Prihanditya and Alamsyah 2020):

$$v' = \frac{v_i - E_i}{std\ (E)} \qquad (2)$$

where v' and v_i are result of normalization value dan the value to be normalized, E_i is the mean value and $std\ (E)$ is standard deviation.

2.3 Second Derivative of PPG

Perform the calculation of the second derivative of the PPG signal to obtain the ECG signal using the following equation.

$$f' = \frac{f_{ppg}(x_{i+1}) - f_{ppg}(x_{i-1})}{2h} + O(h^2) \qquad (3)$$

$$f'' = \frac{f'^{(x_{i+1})} - f'(x_{i-1})}{2h} + O(h^2) \qquad (4)$$

where x_i is the i-th data and and h is the distance between the data.

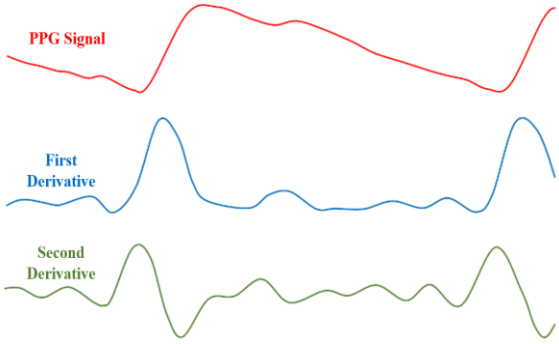

Figure 4: PPG signal and its derivatives

2.4 Linier Normalization (Max)

This method divides the data by its maximum value which is expressed in the following equation (Mathew, Sahu, and Upadhyay 2017):

$$\bar{X}_{ij} = \frac{X_{ij}}{X_j^{Max}} \qquad (5)$$

where X_j^{Max} is the maximum amplitude of the signal. At this stage, the signal will be normalized with a maximum amplitude value of 1.

2.5 Feature Extraction

Feature extraction is done by detecting points P, Q, R, S, T, and U using local maximum and local minimum methods. The peak signal (local maximum) is defined as the sample in which the two direct neighbors have a higher amplitude, while the valley signal (local minimum) is the sample in which the two direct neighbors have a lower amplitude. The features used are the amplitude and duration of the wave.

2.6 Feature Validation

Feature validation is done by comparing the results of PPG signal processing with the value of the ECG signal feature on normal subjects. There are eight features used as shown in the Table I.

Table 1: Feature Value of Normal ECG (L. Wang et al. 2009)

Feature	Value
PR Interval	0.12-0.20 s
P-wave Interval	0.00-0.12 s
QRS	0.06-0.11 s
RR Interval	0.60-1.00 s
R-wave Amplitude	>0.50 mV
QT Interval	0.33-0.43 s
T-wave Amplitude	>0.05 mV
P-wave Amplitude	<0.25 mV

Features obtained from PPG signal processing results that are within feature value of normal ECG range are considered valid, while those outside this range are considered invalid. The statistical analysis includes calculating the mean, standard deviation, and confidence interval for each feature.

3 Result and Discussion

In this study, a comparison was made between the results of PPG signal processing and the features of the ECG signal. This aims to determine whether the ECG graph can be generated through PPG signal processing. The main method used in this study to produce the ECG graphs is the second derivative of the PPG signal or known as the acceleration plethysmogram (APG) (Shahrbabaki et al. 2016). The following is a graph of the results of PPG signal processing on a normal subject as shown in (Figure 5)

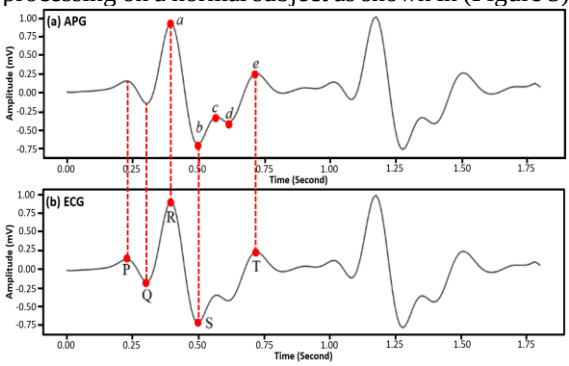

Figure 5: Results of PPG Signal Processing (a) in terms of APG Signals (b) in terms of the ECG Graph

The results of PPG signal processing in Figure 5(a) show the APG signal where the subject is in good circulation. This is because the amplitude of *b*-wave is lower than *c*-wave (Chatterjee and Roy 2018)

A. *P-Wave*

The first deflection of the cardiac cycle is the P-wave caused by depolarization of the right and left atria. The waveform begins as the deflection leaves baseline and ends when the deflection returns to baseline (Huff 2011). In Figure 5, the P-wave corresponds to the peak that appeared before the occurrence of the a-wave on the PPG graph.

B. *PR-Interval*

The PR interval represents the time from the onset of atrial depolarization to the onset of ventricular depolarization (Huff 2011). The PR Interval includes a P-wave and the PR segment (normally is flat/isoelectric, but it may be slightly depressed or downsloping) (Wesley MD 2021). The PR interval is measured from the beginning of the P wave as it leaves baseline to the beginning of the QRS complex (Huff 2011). In Figure 5, the PR interval starts from the P-wave followed by a downsloping PR segment.

C. *QRS-Complex*

The QRS complex represents depolarization of the right and left ventricles. The QRS complex is larger than the P-wave because depolarization of the ventricles involves a larger muscle mass than depolarization of the atria. The QRS complex is composed of three wave deflections: the Q-wave, the R-wave, and the S-wave. The R-wave is a positive waveform; the Q-wave is a negative waveform that precedes the R-wave; the S-wave is a negative waveform that follows the R-wave. The QRS complex is measured from the beginning of the QRS complex (as the first wave of the complex leaves baseline) to the end of the QRS complex (when the last wave of the complex begins to level out into the

ST segment) (Huff 2011). In Figure 5, the Q-wave on the ECG graph corresponds to the valley that appears before the a-wave in the APG signal, the R-wave on the ECG graph corresponds to the b-wave of the APG signal, and the S-wave on the ECG graph corresponds to the c-wave of the APG signal.

D. *T-Wave*

The T wave represents ventricular repolarization. The normal T wave begins as the deflection gradually slopes upward from the ST segment, and ends when the waveform returns to baseline (Huff 2011). In Fig. 5, T-wave corresponds to the e-wave of the APG signal.

E. *RR-Interval*

RR Interval normally represents one cardiac cycle, during with the atria and ventricles contract and relax once. Generally, considered to begin at the peak of one R-wave. Ends at the peak of the next R-wave (Wesley MD 2021). Based on the theoretical review, The RR interval in the ECG correlates closely with the aa interval in the APG signal, as both represent a completed heart cycle (Elgendi 2023). This is in accordance with the results obtained in Figure 5.

The following is the result of PPG signal processing compared to the feature value of the normal ECG for all subjects (shown in Table 2).

Table 2: Comparison Results

ECG Features	Number of Subjects	
	Valid	Invalid
PR Interval	15	10
P-wave Interval	21	4
QRS Complex	0	25
RR Interval	25	0
R-wave Amplitude	25	0
QT Interval	0	25
T-wave Amplitude	25	0
P-wave Amplitude	25	0

In Table 2, "valid" means that the PPG signal processing result corresponds to the feature value of the normal ECG and "invalid" means that the PPG signal processing result does not correspond to the feature value of the normal ECG. Based on the results obtained, there are 4 ECG features (RR Interval, R-wave amplitude, T-wave amplitude, and P-wave amplitude) where all subjects correspond to the results of PPG signal processing. Whereas the ECG features where all subjects did not correspond to the results of PPG signal processing are QRS complex and QT Interval. Meanwhile, the P-wave interval feature consists of 21 "valid" subjects and 4 "invalid" subjects. The PR interval feature consists of 15 "valid" subjects and 10 "invalid" subjects. The results of the statistical analysis are shown in Table 3.

Table 3: Statistical Analysis

Feature	Mean ± SD	CI 95% (Lower and Upper)
PR Interval	0.12 ±0.02	0.11-0.12
P-wave Interval	0.14 ±0.18	0.07-0.21
QRS Complex	0.30 ±0.02	0.29-0.31
RR Interval	0.74 ±0.10	0.70-0.78
R-wave Amplitude	0.95 ±0.08	0.92-0.98
QT Interval	0.52 ±0.04	0.50-0.53
T-wave Amplitude	0.19 ±0.08	0.16-0.22
P-wave Amplitude	0.11 ±0.04	0.09-0.12

The statistical analysis shown in Table 3 provides valuable insights into the reliability and consistency of ECG feature extraction from PPG signal processing. For features with high validity across subjects (RR Interval, R-wave amplitude, T-wave amplitude, and P-wave amplitude), the confidence intervals are relatively narrow, indicating good consistency and reliability in the measurements. For instance, the RR Interval shows a 95% confidence interval of 0.70-0.78 seconds, which falls well within the normal range for healthy subjects (0.60-1.00 seconds). This suggests that PPG-derived RR intervals are highly reliable indicators of cardiac cycle length, which aligns with findings from Gil et al. (2010) who reported strong correlation between PPG and ECG-derived heart rate variability.

The P-wave interval demonstrates a wider confidence interval (0.07-0.21 seconds) compared to other features, with a mean of 0.14 ±0.18 seconds. This wider variation likely contributes to the presence of four invalid subjects in this category. The upper bound of this confidence interval exceeds the normal range (0.00-0.12 seconds), indicating potential challenges in precisely identifying P-wave boundaries from PPG derivatives. This variability may be attributed to the fact that atrial electrical activity, which generates the P-wave in ECG, has a more subtle hemodynamic effect that can be difficult to capture consistently in peripheral blood volume changes detected by PPG (Charlton et al. 2022).

For features with complete invalidity across all subjects (QRS complex and QT interval), the statistical analysis reveals systematic deviations from normal ECG ranges. The QRS complex derived from PPG processing shows a mean of 0.30 ±0.02 seconds with a tight confidence interval (0.29-0.31 seconds), which is significantly longer than the normal ECG range (0.06-0.11 seconds). This substantial difference

suggests fundamental limitations in capturing the rapid ventricular depolarization represented by the QRS complex using PPG-derived methods. Similarly, the QT interval shows a mean of 0.52 ±0.04 seconds (CI: 0.50-0.53 seconds), consistently exceeding the normal range (0.33-0.43 seconds).

The PR interval demonstrates mixed results with 15 valid and 10 invalid subjects. Its mean value (0.12 ±0.02 seconds) falls at the lower bound of the normal range (0.12-0.20 seconds) with a relatively narrow confidence interval (0.11-0.12 seconds). This suggests that while PPG-derived PR intervals can be valid for many subjects, they tend toward the lower end of normal ranges and may underestimate the actual PR interval in some individuals.

These statistical findings align with the physiological basis of cardiac electrical and mechanical activity. Features that represent major hemodynamic events with significant blood volume changes (such as ventricular contraction reflected in R-wave amplitude) show high validity. Conversely, features representing primarily electrical phenomena with subtle hemodynamic effects (such as the QRS complex representing ventricular depolarization) show poor correlation between the PPG-derived ECG and the reference ECG.

The differences observed between ECG and PPG-derived features can be attributed to the fundamental distinction in what these modalities measure. While ECG directly captures the electrical activity of the heart, PPG measures the subsequent mechanical response in peripheral blood vessels. This electromechanical delay, combined with wave propagation effects in the vascular system, introduces temporal distortions that affect certain features more significantly than others. Additionally, the second derivative of PPG (SDPPG) enhances the detection of inflection points in the original waveform but may also amplify noise and artifacts. This could contribute to the inconsistencies observed in features like PR interval and P-wave interval. The strong performance of amplitude-related features (R-wave, T-wave, and P-wave amplitudes) suggests that relative magnitude relationships in the SDPPG signal are well-preserved and correlate well with their ECG counterparts after appropriate normalization.

The existence of ECG features that are not in accordance with the results of PPG signal processing may be due to the fundamental difference between the ECG and PPG principles. ECG represents the electrical signal that comes from the contraction of the heart muscles (Brás et al. 2018), while PPG represents the variations in blood volume or blood flow in the body (Panda, Pinisetty, and Roop 2022). However, ECG indirectly representing the flow of blood inside the heart (Brás et al. 2018).

Our statistical analysis supports the conclusion that while PPG-derived methods cannot fully replace standard 12-lead ECG for comprehensive cardiac assessment, they can reliably extract specific features that are clinically relevant for monitoring purposes. This has significant implications for wearable health monitoring technologies, where PPG sensors are more practical and user-friendly than multi-lead ECG systems.

4 Conclusions

Comparison results of PPG signal processing with ECG normal feature between valid and invalid are PR interval (15:10), P-wave interval (21:4), QRS complex (0:25), RR interval (25:0), R-wave amplitude (25:0), QT interval (0:25), T-wave amplitude (25:0), and P-wave amplitude (25:0). Statistical analysis provides strong support for the validity of specific features, with RR interval (mean: 0.74 ±0.10 s), R-wave amplitude (mean: 0.95 ±0.08 mV), T-wave amplitude (mean: 0.19 ±0.08 mV), and P-wave amplitude (mean: 0.11 ±0.04 mV) all showing consistent correlation between PPG signal processing and ECG measurements. The P-wave interval (mean: 0.14 ±0.18 s) demonstrates high but not complete validity, while PR interval (mean: 0.12 ±0.02 s) shows moderate agreement. In contrast, QRS complex (mean: 0.30 ±0.02 s) and QT interval (mean: 0.52 ±0.04 s) consistently fall outside normal ECG ranges, indicating fundamental limitations in deriving these specific electrical events from PPG signals.

Thus, it can be concluded that while PPG signal processing cannot fully replace standard ECG for comprehensive cardiac assessment, it can reliably extract specific ECG features with high accuracy. The findings demonstrate that PPG-derived methods can effectively reproduce the following ECG parameters: P-wave interval, RR interval, R-wave amplitude, T-wave amplitude, and P-wave amplitude. These results have significant implications for the development of more accessible and user-friendly cardiovascular monitoring technologies that could complement traditional ECG in various healthcare settings

REFERENCES

Ahmed, Solaiman, Tanveer Ahmed Bhuiyan, and Manabu Nii. 2022. “PPG Signal Morphology-Based Method for Distinguishing Stress and Non-Stress Conditions.” *Journal of Advanced*

Computational Intelligence and Intelligent Informatics 26 (1): 58–66. https://doi.org/10.20965/jaciii.2022.p0058.

Benfenati, Luca, Sofia Belloni, Alessio Burrello, Panagiotis Kasnesis, Xiaying Wang, Luca Benini, Massimo Poncino, Enrico Macii, and Daniele Jahier Pagliari. 2024. "EnhancePPG: Improving PPG-Based Heart Rate Estimation with Self-Supervision and Augmentation." arXiv. https://doi.org/10.48550/arXiv.2412.17860.

Brás, Susana, Jacqueline H. T. Ferreira, Sandra C. Soares, and Armando J. Pinho. 2018. "Biometric and Emotion Identification: An ECG Compression Based Method." *Frontiers in Psychology* 9 (April). https://doi.org/10.3389/fpsyg.2018.00467.

Castaneda, Denisse, Aibhlin Esparza, Mohammad Ghamari, Cinna Soltanpur, and Homer Nazeran. 2018. "A Review on Wearable Photoplethysmography Sensors and Their Potential Future Applications in Health Care." *International Journal of Biosensors & Bioelectronics* 4 (4): 195–202. https://doi.org/10.15406/ijbsbe.2018.04.00125.

Chakraborty, Abhishek, Deboleena Sadhukhan, Saurabh Pal, and Madhuchhanda Mitra. 2020. "PPG-BASED AUTOMATED ESTIMATION OF BLOOD PRESSURE USING PATIENT-SPECIFIC NEURAL NETWORK MODELING. | EBSCOhost." August 1, 2020. https://doi.org/10.1142/S0219519420500372.

Charlton, Peter H., Birutė Paliakaitė, Kristjan Pilt, Martin Bachler, Serena Zanelli, Dániel Kulin, John Allen, et al. 2022. "Assessing Hemodynamics from the Photoplethysmogram to Gain Insights into Vascular Age: A Review from VascAgeNet." *American Journal of Physiology-Heart and Circulatory Physiology* 322 (4): H493–522. https://doi.org/10.1152/ajpheart.00392.2021.

Chatterjee, Ayan, and Uttam Kumar Roy. 2018. "Non-Invasive Heart State Monitoring an Article on Latest PPG Processing." *Biomedical and Pharmacology Journal* 11 (4): 1885–93.

Chen, Yung-Sheng, Yi-Ying Lin, Chun-Che Shih, and Cheng-Deng Kuo. 2021. "Relationship Between Heart Rate Variability and Pulse Rate Variability Measures in Patients After Coronary Artery Bypass Graft Surgery." *Frontiers in Cardiovascular Medicine* 8 (December). https://doi.org/10.3389/fcvm.2021.749297.

Elgendi, Mohamed. 2023. *PPG Signal Analysis*. 1st edition. CRC Press.

Elgendi, Mohamed, Yongbo Liang, and Rabab Ward. 2018. "Toward Generating More Diagnostic Features from Photoplethysmogram Waveforms." *Diseases* 6 (1): 20. https://doi.org/10.3390/diseases6010020.

Gil, E, M Orini, R Bailón, J M Vergara, L Mainardi, and P Laguna. 2010. "Photoplethysmography Pulse Rate Variability as a Surrogate Measurement of Heart Rate Variability during Non-Stationary Conditions." *Physiological Measurement* 31 (9): 1271. https://doi.org/10.1088/0967-3334/31/9/015.

Hammad, Mohamed, Asmaa Maher, Kuanquan Wang, Feng Jiang, and Moussa Amrani. 2018. "Detection of Abnormal Heart Conditions Based on Characteristics of ECG Signals." *Measurement* 125 (September):634–44. https://doi.org/10.1016/j.measurement.2018.05.033.

Hartmann, Vera, Haipeng Liu, Fei Chen, Qian Qiu, Stephen Hughes, and Dingchang Zheng. 2019. "Quantitative Comparison of Photoplethysmographic Waveform Characteristics: Effect of Measurement Site." *Frontiers in Physiology* 10 (March):198. https://doi.org/10.3389/fphys.2019.00198.

Houghton, Andrew. 2019. *Making Sense of the ECG: A Hands-On Guide*. 5th edition. CRC Press.

Huff, Jane. 2011. *ECG Workout: Exercises in Arrhythmia Interpretation*. 6th edition. Philadelphia: Lippincott Williams & Wilkins.

Iozzia, Luca, Luca Cerina, and Luca Mainardi. 2016. "Relationships between Heart-Rate Variability and Pulse-Rate Variability Obtained from Video-PPG Signal Using ZCA." *Physiological Measurement* 37 (11): 1934. https://doi.org/10.1088/0967-3334/37/11/1934.

Jelinek, Herbert F., David J. Cornforth, and Ahsan H. Khandoker, eds. 2017. *ECG Time Series Variability Analysis: Engineering and Medicine*. 1st edition. Boca Raton London New York: CRC Press.

Khincha, Rishab, Soundarya Krishnan, Rizwan Parveen, and Neena Goveas. 2020. "ECG Signal Analysis on an Embedded Device for Sleep Apnea Detection." In *Image and Signal Processing*, edited by Abderrahim El Moataz, Driss Mammass, Alamin Mansouri, and Fathallah Nouboud, 377–84. Cham: Springer International Publishing. https://doi.org/10.1007/978-3-030-51935-3_40.

Krishnan, Sridhar. 2021. *Biomedical Signal Analysis for Connected Healthcare*. 1st edition. London: Academic Press.

Liang, Yongbo, Zhencheng Chen, Rabab Ward, and Mohamed Elgendi. 2018. "Hypertension Assessment via ECG and PPG Signals: An Evaluation Using MIMIC Database." *Diagnostics* 8 (3): 65.

https://doi.org/10.3390/diagnostics8030065.

Mathew, Manoj, S. Sahu, and A. Upadhyay. 2017. "Effect Of Normalization Techniques In Robot Selection Using Weighted Aggregated Sum Product Assessment." In . https://www.semanticscholar.org/paper/Effect-Of-Normalization-Techniques-In-Robot-Using-Mathew-Sahu/d47cbb3052130e82a8a2ba69db90fa005db5435a.

Mishra, Bhanupriya, and Neelam Sobha Nirala. 2020. "A Survey on Denoising Techniques of PPG Signal." In *2020 IEEE International Conference for Innovation in Technology (INOCON)*, 1–8. https://doi.org/10.1109/INOCON50539.2020.9298358.

Mukhyber, Sondos Jameel 1, Dhahir Abdulhade 1 Abdulah, and Amer D. 2 1 Department of Computer Science College of Science Majeed. 2021. "Effect Z-Score Normalization on Accuracy of Classification of Liver Disease," 658–62.

Neha, H. K. Sardana, R. Kanwade, and S. Tewary. 2021. "Arrhythmia Detection and Classification Using ECG and PPG Techniques: A Review." *Physical and Engineering Sciences in Medicine* 44 (4): 1027–48. https://doi.org/10.1007/s13246-021-01072-5.

Panda, Abhinandan, Srinivas Pinisetty, and P. Roop. 2022. "Runtime Monitoring and Statistical Approaches for Correlation Analysis of ECG and PPG." *ArXiv*, January. https://doi.org/10.48550/arXiv.2202.00559.

Podaru, Alexandru Constantin, and Valeriu David. 2020. "Blood Pressure Estimation Based on Synchronous ECG and PPG Recording." In *2020 International Conference and Exposition on Electrical And Power Engineering (EPE)*, 640–45. https://doi.org/10.1109/EPE50722.2020.9305544.

Prihanditya, Hestu Aji, and Alamsyah. 2020. "The Implementation of Z-Score Normalization and Boosting Techniques to Increase Accuracy of C4.5 Algorithm in Diagnosing Chronic Kidney Disease." *Journal of Soft Computing Exploration* 1 (1): 63–69. https://doi.org/10.52465/joscex.v1i1.8.

Sattar, Yasar, and Lovely Chhabra. 2025. "Electrocardiogram." In *StatPearls*. Treasure Island (FL): StatPearls Publishing. http://www.ncbi.nlm.nih.gov/books/NBK549803/.

Scardulla, Francesco, Gloria Cosoli, Susanna Spinsante, Angelica Poli, Grazia Iadarola, Riccardo Pernice, Alessandro Busacca, Salvatore Pasta, Lorenzo Scalise, and Leonardo D'Acquisto. 2023. "Photoplethysmograhic Sensors, Potential and Limitations: Is It Time for Regulation? A Comprehensive Review." *Measurement* 218 (August):113150. https://doi.org/10.1016/j.measurement.2023.113150.

Shahrbabaki, Sobhan Salari, Beena Ahmed, Thomas Penzel, and Dean Cvetkovic. 2016. "Photoplethysmography Derivatives and Pulse Transit Time in Overnight Blood Pressure Monitoring." In *2016 38th Annual International Conference of the IEEE Engineering in Medicine and Biology Society (EMBC)*, 2855–58. https://doi.org/10.1109/EMBC.2016.7591325.

Wang, Li-ping, Mi Shen, Jia-fei Tong, and Jun Dong. 2009. "An Uncertainty Reasoning Method for Abnormal ECG Detection." In *2009 IEEE International Symposium on IT in Medicine & Education*, 1:1091–96. https://doi.org/10.1109/ITIME.2009.5236239.

Wang, Wen-Fong, Ching-Yu Yang, and Yan-Fu Wu. 2018. "SVM-Based Classification Method to Identify Alcohol Consumption Using ECG and PPG Monitoring." *Personal and Ubiquitous Computing* 22 (2): 275–87. https://doi.org/10.1007/s00779-017-1042-0.

Wesley MD, Keith. 2021. *Huszar's ECG and 12-Lead Interpretation*. 6th edition. Philadelphia: Elsevier.

Wong, Mark Kei Fong, Hao Hei, Si Zhou Lim, Eddie Yin-Kwee Ng, Mark Kei Fong Wong, Hao Hei, Si Zhou Lim, and Eddie Yin-Kwee Ng. 2023. "Applied Machine Learning for Blood Pressure Estimation Using a Small, Real-World Electrocardiogram and Photoplethysmogram Dataset." *Mathematical Biosciences and Engineering* 20 (1): 975–97. https://doi.org/10.3934/mbe.2023045.

Zeng, Rui, ed. 2015. *Graphics-Sequenced Interpretation of ECG*. 1st ed. 2016 edition. Singapore: Springer.

Zeynali, Mahdi, Khalil Alipour, Bahram Tarvirdizadeh, and Mohammad Ghamari. 2025. "Non-Invasive Blood Glucose Monitoring Using PPG Signals with Various Deep Learning Models and Implementation Using TinyML." *Scientific Reports* 15 (1): 581. https://doi.org/10.1038/s41598-024-84265-8.

Zhang, Dongdong, Samuel Yang, Xiaohui Yuan, and Ping Zhang. 2021. "Interpretable Deep Learning for Automatic Diagnosis of 12-Lead Electrocardiogram." *iScience* 24 (4): 102373. https://doi.org/10.1016/j.isci.2021.102373.

Zheng, Jianwei, Jianming Zhang, Sidy Danioko, Hai Yao, Hangyuan Guo, and Cyril Rakovski. 2020.

"A 12-Lead Electrocardiogram Database for Arrhythmia Research Covering More than 10,000 Patients." *Scientific Data* 7 (1): 48. https://doi.org/10.1038/s41597-020-0386-x.

BIOGRAPHY

Hilman Asyrafi is a lecturer at Politeknik Negeri Media Kreatif, Indonesia. He completed his Master's degree in Engineering Physics at Universitas Gadjah Mada, Indonesia. His research focuses on biosignal processing, instrumentation, and artificial intelligence, with an emphasis on developing adaptive solutions in medical and cognitive technology.

Sunarno is a professor at the Department of Nuclear Engineering and Engineering Physics, Universitas Gadjah Mada, Indonesia, and a consultant in the Medical Instrumentation Division at UPH-LERES. He earned his doctoral degree in Nuclear Electronics from Osaka University, Japan. His research includes high-performance RF filters, human balance monitoring systems, and medical devices. He is actively involved in the development of digital-based diagnostic tools.

Memory Motivanisman Waruwu is a research coordinator at the Laboratory of Sensor and Telecontrol Systems, Universitas Gadjah Mada. He completed his Master of Engineering at Universitas Gadjah Mada, Indonesia. His research interests include sensors, telecontrol, medical devices, and industrial safety, with a focus on physiological monitoring systems.

Rony Wijaya is an engineering manager at PT Datto Asia Teknologi. He completed his Master's degree in Industrial Safety Engineering at Universitas Gadjah Mada, Indonesia. His work involves safety systems, medical technology, and simulation-based training tools for healthcare and industry.